

# ELECTROSTATICS-DEPENDENT SHAPE OF THE INTRINSICALLY-DISORDERED PROTEIN Sic1: How Big Is It? What Does It Look Like?

BY GREGORY-NEAL W. GOMES, BAOXU LIU, VERONIKA CSIZMOK, JULIE FORMAN-KAY, AND CLAUDIU C. GRADINARU

Many eukaryotic proteins contain unstructured segments or completely lack a well-structured three-dimensional fold. These proteins, known as intrinsically disordered proteins (IDPs), exist in dynamic ensembles of conformations<sup>[1,2]</sup>. Although IDPs lack one specific conformation, it is possible to characterize their statistical distribution of conformations, henceforth referred to simply as shape. For IDPs containing a high density of charged residues, there is evidence that an isotropic random coil may be an inadequate shape description<sup>[3,4]</sup>. Accordingly, we used time-resolved fluorescence anisotropy (TRFA), a technique sensitive to the size and shape of the protein by assessing its rotational hydrodynamics, to characterize a highly charged IDP, Sic1.

Sic1 is a 283 residue, highly positively charged IDP in the budding yeast *Saccharomyces Cerevisiae*<sup>[5]</sup>. Its main function is preventing yeast from entering the S phase from the G1 phase of the cell cycle, i.e., preventing DNA replication until the right time<sup>[6]</sup>. To advance to the S phase, Sic1 must be degraded by binding to Cdc (Cell division control)4 protein<sup>[6]</sup>.

The binding affinity of Sic1 for its partner is highly dependent on its phosphorylation state, although the corresponding physical basis is not fully understood. Phosphorylation makes negative contributions to the net charge of Sic1, which decreases from +11 when not phosphorylated, to -1 at threshold phosphorylation. In a model proposed by Forman-Kay and her coworkers, phosphorylated Sic1 (pSic1) and Cdc4 form a dynamic

complex<sup>[7]</sup>. Multiple phosphorylated binding sites on Sic1 weakly interact with Cdc4's positively charged binding pocket. Non-bound charges at any given instant contribute to a mean electrostatic field, producing a mean-field statistical model. This suggests pSic1 will be compact to achieve cumulative electrostatic interaction and to avoid solvent screening effects. The size and shape of Sic1 and pSic1 and the effect of electrostatic interactions (for example charge screening, Fig. 1(b)) is therefore vital to further refine this model.

## THEORY

### Rotational Diffusion

Hydrodynamic properties such as the translational and rotational diffusion coefficients provide information about molecular weight, size, hydration, shape, flexibility, conformation and binding of the protein. Consider the simplest shape, a rigid sphere, perhaps representing a hydrated globular protein. Under randomizing Brownian motion, a correlation time,  $\Phi_{sphere}$ , inversely proportional to the rotational diffusion coefficient,  $D_{rot}$ , describes the exponential decay, or relaxation, of a function of the orientation<sup>[8]</sup>.

The Stokes-Einstein-Debye equation (Equation 1) relates  $\Phi_{sphere}$  to the hydrated volume  $V_h$ , and thus the hydrodynamic radius  $R_h$ , and the molecular weight  $M$ <sup>[8]</sup>:

$$\phi_{sphere} = \frac{\eta V}{RT} = \frac{\eta M}{RT} (\bar{v} + h) = \frac{1}{6D_{rot}} = \frac{V_h \eta}{kT} = \frac{4\pi \eta R_h^3}{3k_B T}$$

where  $\bar{v}$  is the specific volume of the protein,  $h$  is the hydration, and  $\eta$  is the viscosity of the solvent.

This correlation time is for a *rigid spherical* rotator. For non-spherical cases, the rotational diffusion is anisotropic with tensor properties<sup>[8,9,10]</sup>. Non-spherical shapes are often effectively modeled as ellipsoids. The simplest ellipsoids, ellipsoids of revolution, have one unique axis, two equivalent axes, and two rotational diffusion coefficients; about the unique ( $D_{||}$ ) and perpendicular to the unique axes ( $D_{\perp}$ ) (Fig. 1 (a))<sup>[8,9,10]</sup>. A prolate



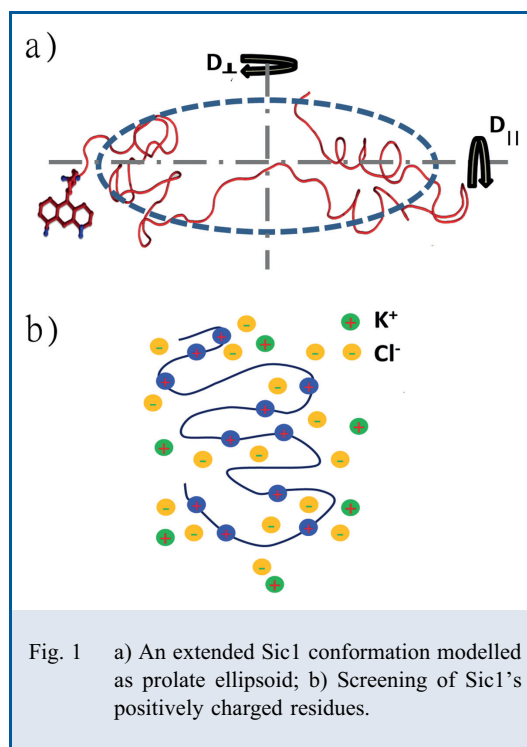
Gregory-Neal W. Gomes, Baoxu Liu, Claudiu C. Gradinaru <claudiu.gradinaru@utoronto.ca>, Dept. of Physics, University of Toronto, and Department of Chemical and Physical Sciences, University of Toronto Mississauga, Mississauga, Ontario L5L 1C6, Canada

and

Veronika Csizmok, Julie Forman-Kay, Molecular Structure and Function Program, Hospital for Sick Children, Toronto, Ontario M5S 1A8 and Dept. of Biochemistry, University of Toronto, Toronto Ontario M5G 1X8, Canada

## SUMMARY

**Time-resolved fluorescence anisotropy (TRFA) measurements are used to probe electrostatics-dependent size and shape of an intrinsically disordered protein (IDP) Sic1.**



ellipsoid has a unique axis longer than the two equivalent axes. Importantly one does not directly measure  $D_{\parallel}$  and  $D_{\perp}$ , but rather the correlation times, a function of  $D_{\parallel}$  and  $D_{\perp}$ .

#### Time-Resolved Fluorescence Anisotropy

In fluorescence anisotropy experiments, the orientation of molecules is probed using polarized light. The anisotropy decay is defined as the difference between the fluorescence intensity emitted parallel,  $I_{\parallel}$ , and perpendicular,  $I_{\perp}$ , to the excitation polarization, normalized by the total intensity<sup>[9]</sup>:

$$r(t) = \frac{I_{\parallel}(t) - I_{\perp}(t)}{I_{\parallel}(t) + 2I_{\perp}(t)}$$

For a sphere the decay is mono-exponential and the correlation time is directly related to  $D_{rot}$ <sup>[9]</sup>:

$$r(t) = r_0 e^{\frac{-t}{D_{rot}}} = r_0 e^{-6D_{rot}t}$$

For a prolate ellipsoid, the anisotropy decay is a tri-exponential, with the amplitudes depending on the angle between the transition dipole and the unique axis<sup>[9]</sup>:

$$r(t) = r_1 e^{\frac{-t}{\phi_{ellips,1}}} + r_2 e^{\frac{-t}{\phi_{ellips,2}}} + r_3 e^{\frac{-t}{\phi_{ellips,3}}}$$

with the three ellipsoidal correlation times  $\phi_{ellips,1-3}$  being functions of  $D_{\parallel}$  and  $D_{\perp}$ <sup>[9]</sup>:

$$\begin{aligned}\phi_{ellips,1} &= (D_{\parallel} + 5D_{\perp})^{-1} \\ \phi_{ellips,2} &= (4D_{\parallel} + 2D_{\perp})^{-1} \\ \phi_{ellips,3} &= (6D_{\perp})^{-1}\end{aligned}$$

For a fluorophore attached to a protein, the depolarizing motions include (global) rotations of the protein and (local) dynamics of the fluorophore about the flexible covalent linker. Thus, a bi-exponential decay describes a sphere with flexible linker. Further addition of exponential decays is needed to describe an ellipse with covalent linker. Additional exponential decays are also present if there is segmental flexibility or flexibility of the protein as a whole<sup>[9,11,12,13]</sup>. In practice, no more than three timescales of motion are resolvable<sup>[9,12]</sup>. The fluorescence anisotropy (FA) was directly calculated from  $I_{\parallel}$  and  $I_{\perp}$  using Equation 2 and fit using a sum of exponentials in Origin (OriginLab, Northampton, MA) with nonlinear least squares fitting and the Levenberg-Marquardt algorithm.

From the selection probability of a randomly oriented population of molecules, the fundamental anisotropy  $r_0$  is 0.4 for collinear absorption and emission dipoles<sup>[9]</sup>.

#### EXPERIMENTAL

A Ti: Sapphire laser (Tsunami HP, Spectra Physics) tuned to a center wavelength of 1055 nm outputs femtosecond pulses. These near-infrared pulses are frequency doubled to obtain green light. At an 80 MHz pulse repetition rate, the time interval between pulses is 12.5 ns. A polarizer in the excitation path confirms that the excitation light reaching the sample is linearly polarized. Observations were performed using a custom built multiparameter confocal microscope, described in detail elsewhere<sup>[14]</sup>. The fluorescence is split into  $I_{\parallel}$  and  $I_{\perp}$  and detected using a single photon counting scheme. Seven of Sic1's possible phosphorylation sites are clustered in the 90 residue N-terminal region ( $\sim 10$  kDa) and are sufficient for targeting of Sic1 to Cdc4<sup>[15]</sup> so this fragment is used in our study and labelled with the fluorophore Tetramethylrhodamine (TMR)-maleimide at one of its terminal sites. Correction factors for the high numerical aperture objective lens and dissimilar polarization sensitivities are included, as described elsewhere<sup>[9,16]</sup>.

#### RESULTS

Typical measured intensity decays in a solution with 150 mM salt (KCl) are shown in Fig. 2(a, inset). The calculated FA decay curve is shown in Fig. 2(b) along with the bi-exponential fit of the data. The fitting parameters obtained by fitting the TRFA data for different salt concentrations are summarized in Fig. 2(c) and in Table 1.

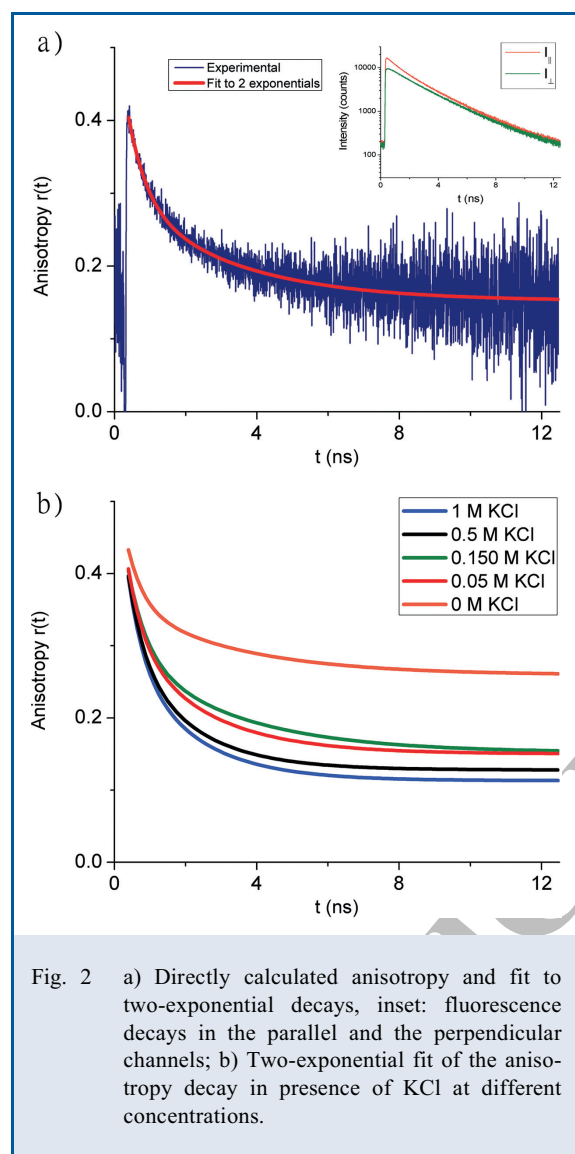


Fig. 2 a) Directly calculated anisotropy and fit to two-exponential decays, inset: fluorescence decays in the parallel and the perpendicular channels; b) Two-exponential fit of the anisotropy decay in presence of KCl at different concentrations.

The model used is

$$r(t) = A_1 e^{-\frac{t-t_0}{\Phi_1}} + A_2 e^{-\frac{t-t_0}{\Phi_2}} + A_3 e^{-\frac{t-t_0}{\Phi_3}}$$

where  $t_0$  is determined experimentally from scattering data and fixed during the fitting, while all other parameters are variable. Three-exponential fits with variable  $\Phi_3$ , converged to a  $\Phi_3$  value on the order of 50 ns but did not converge reproducibly, as this timescale is much longer than the lifetime of the fluorophore ( $\bar{\tau} \approx 4$  ns) and the observation window (12.5 ns). To reduce the uncertainty in the fitting results, the third exponential was fixed to be a constant (by fixing  $\Phi_3$  at infinity). This is justified as positing that a free rotator in solution is unhindered and  $r$  should decay to zero (for long times).

TABLE 1

Sic1 TRFA FITTING RESULTS USING A BI-EXPONENTIAL MODEL. FITTING UNCERTAINTY IS 1–5% IN  $A$ 'S AND 5–10% IN  $\Phi$ 'S.

[KCl] (M)	$r(0)$	$A_1$	$\Phi_1$ (ns)	$A_2$	$\Phi_2$ (ns)	$A_3$	$\Phi_3$ (ns)	$\chi^2_v$
0	0.43	0.094	0.45	0.080	3.1	0.259	$\infty$	0.96
0.05	0.41	0.101	0.44	0.155	2.2	0.150	$\infty$	1.03
0.15	0.40	0.117	0.53	0.135	3.0	0.152	$\infty$	1.03
0.5	0.39	0.10	0.44	0.16	1.7	0.128	$\infty$	0.97
1	0.39	0.11	0.43	0.17	1.8	0.113	$\infty$	0.99

## DISCUSSION

The sub-nanosecond decay of  $\Phi_1$  is comparable with the measured values of the free dye in aqueous solution and is therefore identified as the rotational diffusion of the dye within a cone fixed on the protein surface<sup>[9]</sup>.

The plausibility of a spherical shaped protein can be assessed by comparing the data to the correlation time predicted by eq. 1. Assuming typical values for  $h$ ,  $\bar{v}$ , and  $\eta$ , the calculated rotational correlation time of Sic1 is  $\Phi_{sphere} = 3.9$  ns<sup>[8,9]</sup>. This is on the same order of magnitude as  $\Phi_2$ , however it cannot explain the significant non-decaying fraction. A spherical shape is thus not a plausible model for the shape of Sic1.

The theory of rotational hydrodynamics of ellipsoids of revolution describes the deviations from sphere-like rotation<sup>[8,9,10]</sup>. For axial ratio  $\rho$  (long axis/short axis) between 5 and 10, the longest  $\Phi_{ellips}$  is between 4.64 and 13.37 times longer than  $\Phi_{sphere}$ .<sup>[9]</sup> Rotation displacing the long axis has greater friction, since it displaces more fluid, and it could account for the incomplete decay in our data. For a 10 kDa protein shaped as a prolate ellipsoid with  $5 < \rho < 10$ ,  $\Phi_{ellips,3}$  is between 18 and 52 ns, suggesting a plausible range of  $\rho$  for our data.

It is tempting then to identify  $\Phi_2$  with a remaining rotational correlation time of the ellipsoid. However, one should be circumspect. First, all rotational correlation times of a prolate ellipsoid are greater or roughly equal compared to that of an equivalent volume sphere<sup>[9]</sup>. However,  $\Phi_2$  is less than  $\Phi_{sphere}$  at all salt concentrations. Second, as charge screening decreases, repulsion between charged residues concomitantly decreases  $\rho$ ; and the rotational hydrodynamics should become more sphere-like. Increasing salt concentration,  $\Phi_{ellips,1-3}$  should converge to  $\Phi_{sphere}$ . However,  $\Phi_2$  decreases with increasing salt concentration, further deviating from  $\Phi_{sphere}$ .

A more plausible explanation is that  $\Phi_2$  is due to flexibility of the protein or a segment containing the attached fluorophore. Depolarizing motions from flexibility become less stiff as charge screening attenuates repulsion, producing shorter correlation times, as observed in our data.

## OUTLOOK AND CONCLUSION

What steps are needed to calculate  $\rho$  and semi-axes lengths of the ellipsoid? One challenge is that Sic1 exists in a dynamic ensemble of conformations. Different processes may depolarize each fluorophore due to dissimilar local interactions and motions. One strategy is to use additional fluorescence parameters to resolve sub-populations. Simultaneous acquisition of anisotropy decays and single-molecule Förster Resonance Energy Transfer (sm-FRET) histograms could enable FRET gating of TRFA; the selection of sub-populations with similar conformations for TRFA analysis.

Once the correlation times are confidently attributed to global rotation of the molecule, they must be resolved accurately and

precisely. A study by Wahl<sup>[17]</sup> found the upper-bound of recoverable  $\Phi$  is 10 times the lifetime of the fluorophore,  $\tilde{\tau}$ . Commonly used fluorophores have  $\tilde{\tau} < 5$  ns<sup>[9,11]</sup> so that correlation times of Sic1 with  $\rho > 10$  may not be tractable using TRFA. A viable strategy here is to employ Polarized-FCS (Fluorescence Correlation Spectroscopy). Polarized-FCS is not limited by the fluorescent lifetime and can be used to detect rotational motion on a ns-ms timescale<sup>[18]</sup>.

How big is Sic1? What does it look like? Our anisotropy data suggests a prolate ellipsoid with an axial ratio between 5 and 10, consistent with mutual charge repulsion causing extended chain conformations. Chain flexibility on the same timescale as rotation is also possible. In the future, comparing Sic1 and pSic1 will allow the validation and the improvement of the current model for phosphorylation-dependent activity. We hypothesize that pSic1 will have an aspect ratio closer to unity, so that distal charges are brought closer to the binding pocket, thereby overcoming the solvent screening and achieving a cumulative effect.

## REFERENCES

1. H. J. Dyson and P. E. Wright, "Intrinsically unstructured proteins and their functions", *Nat Rev Mol Cell Biol*, **6**, 197–208, (2005).
2. P. E. Wright and H. J. Dyson, "Linking folding and binding", *Curr. Opin. Struct. Biol.* **19**, 31–38, (2009).
3. A.H. Mao, et al., "Net charge per residue modulates conformational ensembles of intrinsically disordered proteins", *Proc Natl Acad Sci U S A*, **107**, 8183–8188, (2010).
4. B. Liu, et al., "The effect of intrachain electrostatic repulsion on conformational disorder and dynamics of the Sic1 protein", Manuscript in preparation.
5. T. Mittag, et al., "Structure/function implications in a dynamic complex of the intrinsically disordered Sic1 with the Cdc4 subunit of an SCF ubiquitin ligase", *Structure*, **18**, 494–506, (2010).
6. S. Orlicky, et al., "Structural basis for phosphodependent substrate selection and orientation by the SCFCdc4 ubiquitin ligase", *Cell*, **112**, 243–56, 2003.
7. M. Borg, et al., "Polyelectrostatic interactions of disordered ligands suggest a physical basis for ultrasensitivity", *Proc Natl Acad Sci U S A*, **104**, 9650–5, (2007).
8. C.R. Cantor and P.R. Schimmel, *Biophysical Chemistry Part II: Techniques for the Study of Biological Structure and Function*, W.H. Freeman and Company, 1980.
9. J.R. Lakowicz, *Principles of Fluorescence Spectroscopy 3 ed.* Springer Science, 2006.
10. E.W. Small and I. Isenberg, "Hydrodynamic properties of a rigid molecule: Rotational and Linear Diffusion and Fluorescence Anisotropy", *Biopolymers*, **16**, 1907–1928, (1977).
11. E. Feinstein, et al., "Constained analysis of fluorescence anisotropy decay: Application to experimental protein dynamics", *Biophys J*, **84**, 599–611, (2003).
12. S.A. Weinreis, J.P. Ellis and S. Cavagnero, "Dynamic fluorescence depolarization: A powerful tool to explore protein folding on the ribosome", *Methods*, **52**, 57–73, (2010).
13. G.F. Schröder, U. Alexiev, and H. Grubmüller, "Simulation of fluorescence anisotropy experiments: Probing protein dynamics", *Biophys J*, **89**, 3757–3770, (2005).
14. A. Mazouchi, B. Liu, A. Bahram and C. C. Gradinaru, "On the performance of bioanalytical fluorescence correlation spectroscopy measurements in a multiparameter photon-counting microscope", *Anal Chim Acta*, **688**, 61–69, (2011).
15. P. Nash, et al., "Multisite phosphorylation of a CDK inhibitor sets a threshold for the onset of DNA replication", *Nature*, **414**, 514–21, (2001).
16. T. Ha, et al., "Polarization Spectroscopy of Single Fluorescent Molecules", *J Phys Chem B*, **103**, 6839–6850, (1999).
17. P. Wahl, "Analysis of Fluorescence Anisotropy Decays by a Least Square Method", *Bio Phys Chem*, **10**, 91–104, (1979).
18. P. Schwille and E. Haustein, *Fluorescence Correlation Spectroscopy: An introduction to its concepts and applications, The Biophysics Textbook Online.* (2002).